

## State Expansion of a Levitated Nanoparticle in a Dark Harmonic Potential

Eric Bonvin,<sup>1,2</sup> Louisiane Devaud<sup>1,2</sup>, Massimiliano Rossi<sup>1,2</sup>, Andrei Militaru<sup>1,2</sup>, Lorenzo Dania<sup>3</sup>,  
Dmitry S. Bykov<sup>3</sup>, Oriol Romero-Isart<sup>4,5</sup>, Tracy E. Northup<sup>3</sup>, Lukas Novotny,<sup>1,2</sup> and Martin Frimmer<sup>1,2</sup>

<sup>1</sup>Photonics Laboratory, ETH Zürich, 8093 Zürich, Switzerland

<sup>2</sup>Quantum Center, ETH Zürich, Zürich, Switzerland

<sup>3</sup>Department of Experimental Physics, University of Innsbruck, Technikerstraße 25, 6020 Innsbruck, Austria

<sup>4</sup>Department of Theoretical Physics, University of Innsbruck, Technikerstraße 21a, 6020 Innsbruck, Austria

<sup>5</sup>Institute for Quantum Optics and Quantum Information, Austrian Academy of Sciences, Innsbruck, Austria

 (Received 20 December 2023; revised 22 March 2024; accepted 3 May 2024; published 21 June 2024)

We spatially expand and subsequently contract the motional thermal state of a levitated nanoparticle using a hybrid trapping scheme. The particle's center-of-mass motion is initialized in a thermal state (temperature 155 mK) in an optical trap and then expanded by subsequent evolution in a much softer Paul trap in the absence of optical fields. We demonstrate expansion of the motional state's standard deviation in position by a factor of 24. In our system, state expansion occurs devoid of backaction from photon recoil, making this approach suitable for coherent wave function expansion.

DOI: [10.1103/PhysRevLett.132.253602](https://doi.org/10.1103/PhysRevLett.132.253602)

**Introduction.**—Quantum physics predicts that a massive object can be prepared in a macroscopic quantum superposition state. A particularly challenging definition of “macroscopic” in this context requires that the center-of-mass position is delocalized over length scales larger than the physical size of the object [1,2]. The larger the delocalization distance and mass of the object, the more susceptible the state is to external signals and noise, offering advantages for sensing [3,4] and testing quantum mechanics [5,6], including its interplay with gravity [7,8]. Such macroscopic quantum superpositions have been demonstrated with molecules as large as  $10^4$  atomic mass units [9]. Over the past decade, levitated nanoparticles in vacuum [2,10] have emerged as promising candidates to increase the mass of such macroscopic quantum states by at least 4 orders of magnitude [5,11–18]. The first important merit of these levitated systems is that their motional state can be purified by ground-state cooling [19–24]. Their second important merit is that levitation offers the opportunity to manipulate the trapping potential and thereby control the motional state of a levitated object [25–28]. This second merit sets levitated systems apart from clamped optomechanical oscillators [29]. In those systems, impressive optomechanical quantum control has been achieved [30–37], but the length scale set by the zero-point motion of the oscillator cannot be tuned *in situ*.

Control over the trapping potential is a key requirement in both approaches pursued to expand the wave function of a levitated nanoparticle. The first approach relies on purely optical potentials together with free evolution in the absence of a potential [17]. The second approach aims to exploit evolution in a dedicated potential in the absence of decoherence due to measurement backaction inevitably

associated with optical interactions [38–40]. To this end, this strategy proposes to use dark, nonoptical potentials generated by radio-frequency (rf) electric fields [15,18]. In both approaches, state expansion has to occur in the absence of laser light to avoid decoherence due to photon scattering [15,38,39]. On the experimental side, hybrid approaches of optical traps combined with rf (Paul) traps have been investigated [41–47]. Exploiting a hybrid platform for testing expansion protocols on classical states is an outstanding task that would accelerate future progress when moving to the quantum regime.

In this Letter, we expand the classical thermal state of motion of a levitated nanoparticle by transferring it from an optical trap to a weakly confining dark potential implemented with a linear Paul trap. After evolution in the dark potential, the particle is retrapped optically and its position is measured, allowing for repetition of the protocol. We demonstrate a maximum state expansion by a factor of 24 in standard deviation and subsequent contraction to the starting size in addition to a contribution from heating during the protocol. This Letter is an important step toward coherent wave function expansion of levitated nanoparticles in the quantum regime.

**Frequency-jump protocol.**—We start by illustrating the dynamics of a harmonic oscillator with position  $u$  and velocity  $\dot{u}$  under a so-called frequency-jump protocol [4,48–51]. In this protocol, we initialize the oscillator in a thermal state in a (stiff) potential with frequency  $\omega_o$  and period  $T_o$  (in this Letter implemented with an optical trap). With appropriately normalized axes, this initial thermal state is described in phase space by a symmetric Gaussian distribution with widths  $\Delta u_0$  and  $\Delta \dot{u}_0$  along the position and velocity axes, respectively, illustrated in Fig. 1(a).

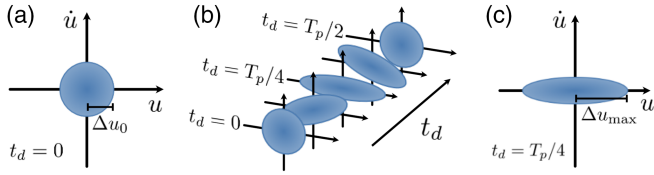


FIG. 1. Phase-space representation of a particle in a harmonic potential undergoing a frequency-jump protocol. (a) The particle is initially in a thermal state, described by a uniform Gaussian distribution of size  $\Delta u_0$ . (b) The state evolves in the weaker potential for increasing  $t_d$ . (c) The maximum size  $\Delta u_{\max}$  is reached for  $t_d = T_p/4$ .

At time  $t = 0$ , we switch to a weaker potential with frequency  $\omega_p < \omega_o$  and period  $T_p$  (implemented with a Paul trap in the absence of laser light) for a time  $t_d$ . The evolution of the state in the weaker potential as a function of  $t_d$  is illustrated in Fig. 1(b). As  $t_d$  increases, the state expands spatially until reaching a maximum size  $\Delta u_{\max}$  for  $t_d = T_p/4$ , as shown in Fig. 1(c). As  $t_d$  increases further, the spatial state size returns to its initial value, reached at  $t_d = T_p/2$ . To characterize the phase-space distribution acquired at time  $t_d$ , we instantaneously switch the potential back to frequency  $\omega_o$ . Now, the state rotates in phase space with preserved shape. In this Letter, we experimentally realize this frequency-jump protocol in a hybrid Paul-optical trap.

**Experimental setup.**—Our setup overlaps an optical trap with a linear Paul trap, in which we levitate a 177 nm diameter silica nanosphere. This configuration, shown in Fig. 2, allows us to selectively trap the same particle in either trap. What follows is a simplified description of the setup (further details in Ref. [52]).

The optical trap is generated by a laser ( $x$ -polarized, wavelength 1565 nm, power 500 mW) focused by a lens (NA = 0.77, optical axis along  $z$ ). The particle's center-of-mass oscillation frequencies are  $2\pi \times (44, 58, 10)$  kHz along  $(x, y, z)$ , respectively. The trap can be switched on and off with an acousto-optic modulator on a timescale faster than 100 ns. The forward scattered light is collected by an identical lens, and sent onto a quadrant photodiode for position detection in the  $(x, y, z)$  basis.

The Paul trap consists of a glass substrate micro-machined to a wheel-trap geometry (FEMTOprint, Switzerland) [53–56]. The metallized electrodes are oriented along the orthogonal directions  $u$  and  $v$ , which lie in the focal plane and are tilted at  $45^\circ$  relative to  $x$  and  $y$ . The two pairs of rf electrodes are driven with opposite phases at a frequency of 33 kHz and a nominal peak-to-peak voltage of 400 V. Confinement along  $z$  is achieved by applying a typical end-cap voltage of 70 V to the metallic lens holders. This results in secular center-of-mass modes at  $2\pi \times (6, 6, 3)$  kHz along  $(u, v, z)$ , respectively. The radial and axial mode frequencies can be tuned from 0.1 to 6 kHz by adjusting the applied voltages. The trap is

mounted in a vacuum chamber and kept at a pressure of  $2.2 \times 10^{-6}$  mbar. Before starting our experiments, we compensate for stray fields in the trapping region using the shim electrodes of our trap [52,57].

We execute a frequency-jump protocol by rapidly transferring the particle from the high-frequency optical trap to the lower frequency Paul trap and back. Experimentally, this is achieved by switching the optical trap off and back on, while keeping the Paul trap enabled at all times. More specifically, we execute the following protocol: (i) for  $t < 0$ , the particle is held in the optical trap, and initialized to a feedback-cooled thermal state of motion; (ii) at time  $t = 0$ , feedback cooling is disabled, and the optical trap is rapidly switched off; (iii) for  $0 < t < t_d$ , the particle evolves in the Paul trap until (iv) at  $t = t_d$ , the optical trap is switched back on to recapture the particle optically; and (v) the final position of the particle in phase space is characterized for  $t > t_d$ .

**Results.**—In Fig. 3(a), we show the measured particle position during one realization of this frequency-jump protocol with  $t_d = 72 \mu\text{s}$  (black data points). The measurement of the particle's position for times  $t < 0$  is largely impacted by noise, as expected from a state under feedback cooling. In contrast, the oscillations in the particle's position are clearly visible at the end of the protocol ( $t > 150 \mu\text{s}$ ). We note that for times  $0 < t < t_d$ , no measurement record exists, since the optical field is off. Furthermore, between  $t = 72 \mu\text{s}$  and  $\approx 150 \mu\text{s}$ , we observe a slow recovery of the recorded time trace after re-enabling the optical trap due to ac coupling of the data acquisition system. To avoid unwanted artifacts in our data analysis, we ignore the first 120  $\mu\text{s}$  of signal upon recapture [open data points in Fig. 3(a), see Ref. [58]].

We use the measurement record to retrodict the position and velocity after recapture at  $t = t_d$  in the optical trap (see Supplemental Material [58]). The retrodicted trajectory is shown as the dashed blue line in Fig. 3(a). The phase-space

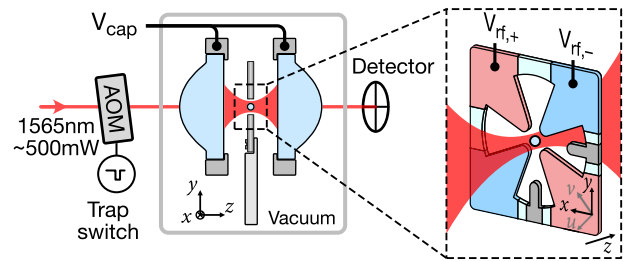


FIG. 2. Experimental setup. A laser beam is focused by a lens to form an optical trap. The trapped particle's center-of-mass motion is recorded on a quadrant photodetector. The laser can be switched on and off with an acousto-optic modulator (AOM). The optical trap is superimposed with a Paul trap. It consists of a microfabricated chip held in the focal plane and end-cap electrodes (held at a potential  $V_{\text{cap}}$ ). The two pairs of on-chip electrodes are driven with rf voltages ( $V_{\text{rf},+}$  and  $V_{\text{rf},-}$ , respectively) for in-plane confinement.

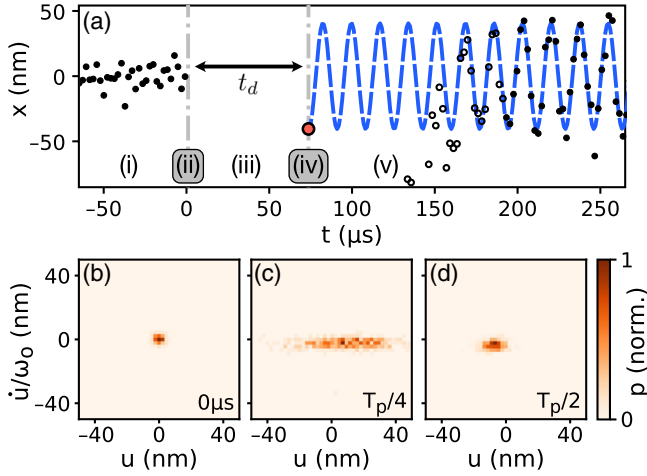


FIG. 3. (a) Recorded position during a single realization of a frequency-jump protocol (black data points, open points not used for data analysis, see main text). The optical trap is disabled from  $t = 0$  to  $t = t_d = 72 \mu\text{s}$ , allowing the particle to evolve in the Paul trap. The oscillation after recapture is fit (dashed blue line) to estimate the position and velocity of the particle at time of recapture  $t = t_d$  (red circle). (b) Initial state of the particle, reconstructed from 500 repetitions of the protocol with  $t_d = 0$  (bin size  $1 \text{ nm} \times 1 \text{ nm}$ ). (c) For  $t_d = 72 \mu\text{s} \approx T_p/4$ , the state has visibly expanded along the position axis. (d) For  $t_d = 140 \mu\text{s} \approx T_p/2$ , the state has contracted back to a size similar to the initial distribution.

distribution before the frequency jump is inferred by retrodicting the phase-space position of the particle for protocols executed with  $t_d = 0$ , i.e., the trapping laser is not switched. Thus, all phase-space distributions are generated using the identical data-processing protocol. Another challenge arises from the coupling of the motion along  $x$  and  $y$  by the electric fields in the Paul trap, which are aligned along the  $u$  and  $v$  axes. Therefore, in the following, we combine the measurements of  $x$  and  $y$  to analyze motion along  $u$ .

A phase-space distribution of the particle before the frequency jump, i.e., at  $t_d = 0$ , retrodicted from 500 repetitions of the experiment, is shown in Fig. 3(b). Each repetition is started at the same time in the micromotion cycle. Here, the particle is cooled to a state size of  $(1.5 \pm 0.1) \text{ nm}$  in the optical trap. This corresponds to a center-of-mass temperature of  $T_{\text{CoM}} = (155 \pm 25) \text{ mK}$ . The state size  $\Delta u$  is defined as the standard deviation of the position  $u$ . We characterize the estimation noise independently and subtract it from the signal when evaluating  $\Delta u$ . The error is evaluated using the bootstrap method [65]. Figure 3(c) shows the distribution after an evolution time  $t_d = 72 \mu\text{s}$ , corresponding to a quarter oscillation period in the Paul trap. In comparison to the initial state, the distribution for  $t_d = 72 \mu\text{s}$  is stretched along the position axis, reaching a state size of  $(26.4 \pm 1.2) \text{ nm}$ . This state expansion in a dark potential

is the main result of this Letter. In Fig. 3(d), we show the distribution for  $t_d = 140 \mu\text{s} \approx T_p/2$ , where the state has contracted to  $\Delta u = (4.4 \pm 0.2) \text{ nm}$ , as expected. The increase in state size during evolution from Figs. 3(b)–3(d) is a signature of heating due to collisions of the particle with gas molecules [38,66,67].

We proceed by investigating the role of the frequency ratio  $r = \omega_o/\omega_p$  (tuned via the voltage of the Paul trap rf drive) in our expansion protocol. Figure 4(a) shows the state size  $\Delta u$  (blue circles) estimated from the measurement data as a function of evolution time  $t_d$  for a frequency ratio  $r = 8.8$ . We identify the following three features. First, the state size grows and shrinks with a period  $T_p/2$ , as expected. Second, we observe a fast modulation whose period matches that of the rf field driving the Paul trap. Third, the minimum of each expansion cycle trends upward, suggesting that the minimal state size continuously grows as a consequence of heating during the expansion protocol.

We investigate these features for larger frequency ratios  $r = 14.6$  and  $r = 24.3$  in Figs. 4(b) and 4(c), respectively. For weaker Paul traps, the main oscillations are slower and of larger amplitude than for stiffer traps. In Fig. 4(c), we achieve a state expansion by a factor of 24 when comparing the size of  $35.6 \text{ nm}$  at  $t_d = 104 \mu\text{s}$  to the initial size of  $1.5 \text{ nm}$ . We observe that weaker Paul traps are less heavily modulated by oscillations at the rf frequency, which we attribute to the lower rf drive voltages. Finally, weaker traps are more sensitive to heating, seen by the more rapid increase of the minima in Fig. 4(c) as compared to Fig. 4(a).

*Discussion.*—To understand our observations, we model the behavior of a particle’s state subject to a frequency-jump protocol. To simplify the description, we assume that the Paul trap is a harmonic potential. A complete model including the effects of micromotion can be found in Ref. [58]. We model the particle in the Paul trap as a harmonic oscillator of mass  $m$  coupled to a thermal bath at rate  $\gamma$ , following the equation of motion

$$\ddot{u} + \omega_p^2 u = \sqrt{2\gamma k_B T/m} \xi_{\text{th}}, \quad (1)$$

where we neglect the damping term (since  $\gamma \ll \omega_p$ ), we assume  $u^2 \ll k_B T/(m\omega_p^2)$ , and each dot represents a time derivative. The bath has temperature  $T$  and is modeled using the stochastic variable  $\xi_{\text{th}}$ , which satisfies  $\langle \xi_{\text{th}}(t) \xi_{\text{th}}(t') \rangle = \delta(t - t')$ . Here,  $\langle \dots \rangle$  denotes an ensemble average. Solving Eq. (1), we find that the spatial state size of the particle, given by the standard deviation  $\Delta u$  after the protocol, evolves according to  $\Delta u^2(t) = \Delta u_c^2(t) + \Delta u_h^2(t)$ . The first contribution stems from coherent evolution and is given by [49]

$$\Delta u_c^2(t) = \Delta u_0^2 \cos^2(\omega_p t) + r^2 \frac{\Delta u_0^2}{\omega_o^2} \sin^2(\omega_p t), \quad (2)$$

with  $\Delta u_0$  the initial state size. The second term of Eq. (2) scales with the ratio of the initial velocity state size  $\Delta \dot{u}_0^2$  and the (square of the) frequency of the Paul trap  $\omega_p^2 = \omega_o^2/r^2$ . When the protocol is started with a thermal state of the optical potential, we have  $\Delta \dot{u}_0/\omega_o = \Delta u_0$  and the maximum spatial state size from coherent evolution is given by  $\Delta u_{c,\max} = r\Delta u_0$ , such that the spatial expansion is simply dictated by  $r$ . The situation in our experiment is slightly more complicated. The particle is initialized in the optical trap in two uncorrelated thermal states along  $x$  and  $y$ . However, we perform our subsequent experiments in the rotated basis  $uv$ . The distributions along  $u$  and  $v$  then become correlated, and the relation  $\Delta \dot{u}_0/\omega_o = \Delta u_0$  no longer holds. For more detail, refer to the Supplemental Material [58]. The second contribution to  $\Delta u^2$  arises from heating and reads

$$\Delta u_h^2(t) = r^2 \frac{\hbar\Gamma}{m\omega_o} \left( t - \frac{\sin(2\omega_p t)}{2\omega_p} \right). \quad (3)$$

Here, to align with the literature [18], we have introduced the heating rate  $\Gamma$ , which is expressed in units of phonons of the optical trapping potential. In our experiment, where heating is dominated by coupling to the residual gas in the vacuum chamber at temperature  $T$ , we have  $\Gamma = \gamma k_B T / (\hbar\omega_o)$ , which we measure to be  $\Gamma = 2\pi \times (926 \pm 56)$  kHz.

Care must be taken when defining the optical trap frequency  $\omega_o$  in Eq. (2). Since we are interested in the particle motion along  $u$ , but the optical trap's eigenmodes are oriented along  $x$ ,  $y$ , and  $z$ , we define the effective oscillation frequency along  $u$  as  $\omega_{u,\text{opt}} = [(\omega_{x,\text{opt}}^2 + \omega_{y,\text{opt}}^2)/2]^{1/2}$ . We fit our model to the measured data using the Paul trap frequency  $\omega_p$  as the only fit parameter. All other parameters ( $\Delta u_0$ ,  $\Delta \dot{u}_0$ ,  $\omega_o$ ,  $\gamma$ , and  $T$ ) are measured independently.

The simplified model is shown in Fig. 4 as the dashed gray lines, while the dotted gray lines show the heating contribution  $\Delta u_h$ . Our simplified model reproduces all features of the data well, except the modulation at the micromotion frequency. In contrast, the full model (solid line in Fig. 4) accounts for all features observed during a frequency-jump protocol. Comparing the two models in Fig. 4(a) reveals that, for stiff Paul traps, the presence of the rf fields almost doubles the expanded state size as compared to a simple frequency jump.

Another important observation is that our simple model explains the increase of the heating contribution with increasing frequency ratio  $r$ , experimentally observed in Fig. 4. Specifically, according to Eq. (3), at compression time  $T_p/2$ , the total state size has no contribution due to coherent evolution, and is given by

$$\Delta u^2(T_p/2) = \Delta u_0^2 + r^2 \frac{\hbar\Gamma}{m\omega_o} \frac{T_p}{2}. \quad (4)$$

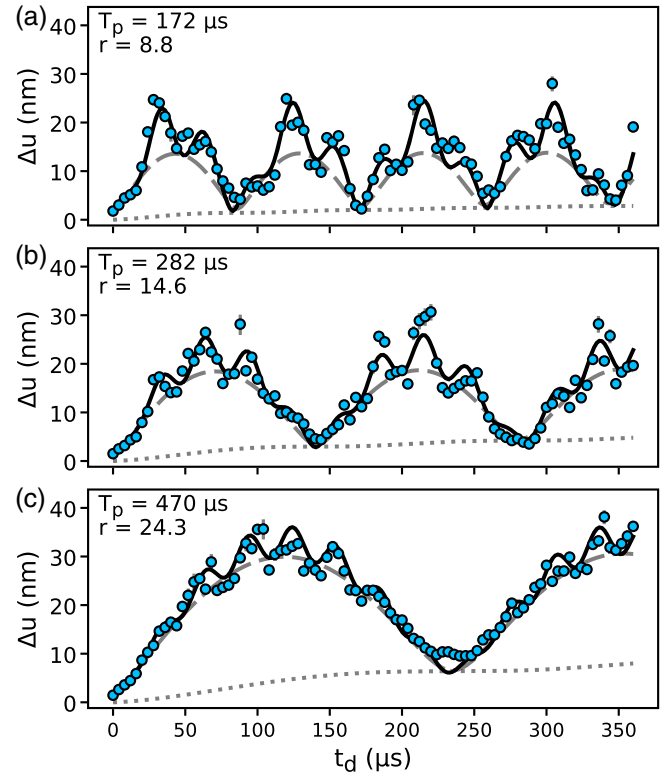


FIG. 4. Measured state size  $\Delta u$  as a function of evolution time  $t_d$  (blue data points), for different Paul trap stiffnesses, quantified by the frequency ratio  $r$ . Solid lines: full model described in the Supplemental Material [58]. Dashed lines: simplified model discussed in the main text. Dotted lines: heating contribution  $\Delta u_h$  under the simplified model.

The only contribution to  $\Delta u^2$  besides the initial value  $\Delta u_0^2$  is from heating. Importantly, the heating rate  $\Gamma$  is amplified by  $r^2$ . This fact can potentially be exploited to measure weak decoherence rates, such as from blackbody emission, which are overwhelmed by photon recoil in optically levitated systems [5,13,68].

Regarding the current limitations of our system, larger expansions could, in principle, be achieved with the help of weaker potentials. However, the associated increase in sensitivity to stray fields leads to frequent failures to recapture the particle in the optical trap and must be overcome with more accurate stray field and gravity compensation in the future.

*Conclusion.*—We have constructed a hybrid Paul-optical trap with high-numerical-aperture optical access, as used in systems achieving measurement-based ground-state cooling of optically levitated nanoparticles [20,21]. Using the large frequency difference between optical and Paul traps, we have expanded and subsequently contracted the thermal state size of an optically levitated nanoparticle by a factor of 24. The expansion happens with the optical tweezer off, i.e., in the absence of photon recoil, which is critical for extending this protocol to generate macroscopic quantum states.

Having demonstrated expansion of a thermal state, a logical next step is to move to ultrahigh vacuum and implement high-efficiency detection [69], unlocking access to ground-state cooling [20–22]. For a ground-state cooled particle in an optical trap, our protocol would expand the state size to about 250 pm, which would be an important step toward a macroscopic quantum state. The enhanced sensitivity to decoherence provided by the protocol may provide a handle to quantify and finally remedy weak sources of decoherence, such as stray fields or black-body radiation. Our protocol is indeed of interest from a quantum sensing perspective. Coherent expansion by a factor of 24 would lead to an unprecedented level of 28 dB of quadrature squeezing in variance, which could be exploited for the detection of weak forces [70,71]. Achieving such squeezing would require decoherence levels in the dark approximately 4 orders of magnitude lower than those associated with photon recoil in an optical trap [3,21]. Returning to the goal of testing quantum mechanics with macroscopic quantum states, the long protocol times associated with simple frequency-jump protocols may, at some level of expansion, prove impractical in presence of inevitable sources of decoherence, such as, e.g., collisions with residual gas molecules [72]. A work-around could be inverted potentials, in which the state expands exponentially fast in time [3,18], significantly reducing required protocol times. Our platform could be used to generate the required inverted quadratic potentials, e.g., by reversing the end-cap voltages.

This research was supported by the Swiss National Science Foundation (SNF) through Grant No. 212599 and No. 217122, NCCR-QSIT program (Grant No. 51NF40-160591), and the European Union’s Horizon 2020 research and innovation program under Grant No. 951234 (Q-Xtreme). This research was funded in whole or in part by the Austrian Science Fund (FWF) [grant DOIs: 10.55776/Y951 and 10.55776/I5540].

---

[1] M. Arndt and K. Hornberger, Testing the limits of quantum mechanical superpositions, *Nat. Phys.* **10**, 271 (2014).  
 [2] C. Gonzalez-Ballester, M. Aspelmeyer, L. Novotny, R. Quidant, and O. Romero-Isart, Levitodynamics: Levitation and control of microscopic objects in vacuum, *Science* **374**, eabg3027 (2021).  
 [3] T. Weiss, M. Roda-Llodes, E. Torrontegui, M. Aspelmeyer, and O. Romero-Isart, Large quantum delocalization of a levitated nanoparticle using optimal control: Applications for force sensing and entangling via weak forces, *Phys. Rev. Lett.* **127**, 023601 (2021).  
 [4] F. Cosco, J. S. Pedernales, and M. B. Plenio, Enhanced force sensitivity and entanglement in periodically driven optomechanics, *Phys. Rev. A* **103**, L061501 (2021).  
 [5] O. Romero-Isart, Quantum superposition of massive objects and collapse models, *Phys. Rev. A* **84**, 052121 (2011).

[6] A. Bassi, K. Lochan, S. Satin, T. P. Singh, and H. Ulbricht, Models of wave-function collapse, underlying theories, and experimental tests, *Rev. Mod. Phys.* **85**, 471 (2013).  
 [7] D. Rickles and C. M. DeWitt, *The Role of Gravitation in Physics: Report from the 1957 Chapel Hill Conference* (Max-Planck-Gesellschaft zur Förderung der Wissenschaften, 2011).  
 [8] A. Belenchia, R. M. Wald, F. Giacomini, E. Castro-Ruiz, i. c. v. Brukner, and M. Aspelmeyer, Quantum superposition of massive objects and the quantization of gravity, *Phys. Rev. D* **98**, 126009 (2018).  
 [9] Y. Y. Fein, P. Geyer, P. Zwick, F. Kiařka, S. Pedalino, M. Mayor, S. Gerlich, and M. Arndt, Quantum superposition of molecules beyond 25 kDa, *Nat. Phys.* **15**, 1242 (2019).  
 [10] J. Millen, T. S. Monteiro, R. Pettit, and A. N. Vamivakas, Optomechanics with levitated particles, *Rep. Prog. Phys.* **83**, 026401 (2020).  
 [11] O. Romero-Isart, A. C. Pflanzner, F. Blaser, R. Kaltenbaek, N. Kiesel, M. Aspelmeyer, and J. I. Cirac, Large quantum superpositions and interference of massive nanometer-sized objects, *Phys. Rev. Lett.* **107**, 020405 (2011).  
 [12] M. Scala, M. S. Kim, G. W. Morley, P. F. Barker, and S. Bose, Matter-wave interferometry of a levitated thermal nano-oscillator induced and probed by a spin, *Phys. Rev. Lett.* **111**, 180403 (2013).  
 [13] J. Bateman, S. Nimmrichter, K. Hornberger, and H. Ulbricht, Near-field interferometry of a free-falling nanoparticle from a point-like source, *Nat. Commun.* **5**, 4788 (2014).  
 [14] C. Wan, M. Scala, G. W. Morley, A. M. Rahman, H. Ulbricht, J. Bateman, P. F. Barker, S. Bose, and M. S. Kim, Free nano-object Ramsey interferometry for large quantum superpositions, *Phys. Rev. Lett.* **117**, 143003 (2016).  
 [15] H. Pino, J. Prat-Camps, K. Sinha, B. P. Venkatesh, and O. Romero-Isart, On-chip quantum interference of a superconducting microsphere, *Quantum Sci. Technol.* **3**, 025001 (2018).  
 [16] B. A. Stickler, B. Papendell, S. Kuhn, B. Schriniski, J. Millen, M. Arndt, and K. Hornberger, Probing macroscopic quantum superpositions with nanorotors, *New J. Phys.* **20**, 122001 (2018).  
 [17] L. Neumeier, M. A. Ciampini, O. Romero-Isart, M. Aspelmeyer, and N. Kiesel, Fast quantum interference of a nanoparticle via optical potential control, *Proc. Natl. Acad. Sci. U.S.A.* **121**, e2306953121 (2024).  
 [18] M. Roda-Llodes, A. Riera-Campeny, D. Candoli, P. T. Grochowski, and O. Romero-Isart, Macroscopic quantum superpositions via dynamics in a wide double-well potential, *Phys. Rev. Lett.* **132**, 023601 (2024).  
 [19] U. Delić, M. Reisenbauer, K. Dare, D. Grass, V. Vuletić, N. Kiesel, and M. Aspelmeyer, Cooling of a levitated nanoparticle to the motional quantum ground state, *Science* **367**, 892 (2020).  
 [20] L. Magrini, P. Rosenzweig, C. Bach, A. Deutschmann-Olek, S. G. Hofer, S. Hong, N. Kiesel, A. Kugi, and M. Aspelmeyer, Real-time optimal quantum control of mechanical motion at room temperature, *Nature (London)* **595**, 373 (2021).  
 [21] F. Tebbenjohanns, M. L. Mattana, M. Rossi, M. Frimmer, and L. Novotny, Quantum control of a nanoparticle optically

- levitated in cryogenic free space, *Nature (London)* **595**, 378 (2021).
- [22] M. Kamba, R. Shimizu, and K. Aikawa, Optical cold damping of neutral nanoparticles near the ground state in an optical lattice, *Opt. Express* **30**, 26716 (2022).
- [23] A. Ranfagni, K. Børkje, F. Marino, and F. Marin, Two-dimensional quantum motion of a levitated nanosphere, *Phys. Rev. Res.* **4**, 033051 (2022).
- [24] J. Piotrowski, D. Windey, J. Vijayan, C. Gonzalez-Ballester, A. de los Ríos Sommer, N. Meyer, R. Quidant, O. Romero-Isart, R. Reimann, and L. Novotny, Simultaneous ground-state cooling of two mechanical modes of a levitated nanoparticle, *Nat. Phys.* **19**, 1009 (2023).
- [25] M. Rashid, T. Tufarelli, J. Bateman, J. Vovrosh, D. Hempston, M. S. Kim, and H. Ulbricht, Experimental realization of a thermal squeezed state of levitated optomechanics, *Phys. Rev. Lett.* **117**, 273601 (2016).
- [26] E. Hebestreit, M. Frimmer, R. Reimann, and L. Novotny, Sensing static forces with free-falling nanoparticles, *Phys. Rev. Lett.* **121**, 063602 (2018).
- [27] M. Frimmer, T. L. Heugel, Ž. Nosan, F. Tebbenjohanns, D. Hälgl, A. Akin, C. L. Degen, L. Novotny, R. Chitra, O. Zilberberg, and A. Eichler, Rapid flipping of parametric phase states, *Phys. Rev. Lett.* **123**, 254102 (2019).
- [28] M. A. Ciampini, T. Wenzl, M. Konopik, G. Thalhammer, M. Aspelmeyer, E. Lutz, and N. Kiesel, Experimental non-equilibrium memory erasure beyond Landauer's bound, [arXiv:2107.04429](https://arxiv.org/abs/2107.04429).
- [29] M. Aspelmeyer, T. J. Kippenberg, and F. Marquardt, Cavity optomechanics, *Rev. Mod. Phys.* **86**, 1391 (2014).
- [30] M. Rossi, D. Mason, J. Chen, Y. Tsaturyan, and A. Schliesser, Measurement-based quantum control of mechanical motion, *Nature (London)* **563**, 53 (2018).
- [31] A. D. O'Connell, M. Hofheinz, M. Ansmann, R. C. Bialczak, M. Lenander, E. Lucero, M. Neeley, D. Sank, H. Wang, M. Weides, J. Wenner, J. M. Martinis, and A. N. Cleland, Quantum ground state and single-phonon control of a mechanical resonator, *Nature (London)* **464**, 697 (2010).
- [32] F. Lecocq, J. B. Clark, R. W. Simmonds, J. Aumentado, and J. D. Teufel, Quantum nondemolition measurement of a nonclassical state of a massive object, *Phys. Rev. X* **5**, 041037 (2015).
- [33] R. Riedinger, S. Hong, R. A. Norte, J. A. Slater, J. Shang, A. G. Krause, V. Anant, M. Aspelmeyer, and S. Gröblacher, Non-classical correlations between single photons and phonons from a mechanical oscillator, *Nature (London)* **530**, 313 (2016).
- [34] C. B. Møller, R. A. Thomas, G. Vasilakis, E. Zeuthen, Y. Tsaturyan, M. Balabas, K. Jensen, A. Schliesser, K. Hammerer, and E. S. Polzik, Quantum back-action-evading measurement of motion in a negative mass reference frame, *Nature (London)* **547**, 191 (2017).
- [35] Y. Chu, P. Kharel, T. Yoon, L. Frunzio, P. T. Rakich, and R. J. Schoelkopf, Creation and control of multi-phonon Fock states in a bulk acoustic-wave resonator, *Nature (London)* **563**, 666 (2018).
- [36] L. R. Sletten, B. A. Moores, J. J. Viennot, and K. W. Lehnert, Resolving phonon Fock states in a multimode cavity with a double-slit qubit, *Phys. Rev. X* **9**, 021056 (2019).
- [37] M. Bild, M. Fadel, Y. Yang, U. von Lüpke, P. Martin, A. Bruno, and Y. Chu, Schrödinger cat states of a 16-microgram mechanical oscillator, *Science* **380**, 274 (2023).
- [38] V. Jain, J. Gieseler, C. Moritz, C. Dellago, R. Quidant, and L. Novotny, Direct measurement of photon recoil from a levitated nanoparticle, *Phys. Rev. Lett.* **116**, 243601 (2016).
- [39] P. Maurer, C. Gonzalez-Ballester, and O. Romero-Isart, Quantum theory of light interaction with a lorenz-mie particle: Optical detection and three-dimensional ground-state cooling, *Phys. Rev. A* **108**, 033714 (2023).
- [40] L. Dania, D. S. Bykov, F. Goschin, M. Teller, A. Kassid, and T. E. Northup, Ultrahigh quality factor of a levitated nanomechanical oscillator, *Phys. Rev. Lett.* **132**, 133602 (2024).
- [41] J. Millen, P. Z. G. Fonseca, T. Mavrogordatos, T. S. Monteiro, and P. F. Barker, Cavity cooling a single charged levitated nanosphere, *Phys. Rev. Lett.* **114**, 123602 (2015).
- [42] P. Nagornykh, J. E. Coppock, and B. E. Kane, Cooling of levitated graphene nanoplatelets in high vacuum, *Appl. Phys. Lett.* **106**, 244102 (2015).
- [43] P. Z. G. Fonseca, E. B. Aranas, J. Millen, T. S. Monteiro, and P. F. Barker, Nonlinear dynamics and strong cavity cooling of levitated nanoparticles, *Phys. Rev. Lett.* **117**, 173602 (2016).
- [44] T. Delord, L. Nicolas, M. Bodini, and G. Hétet, Diamonds levitating in a Paul trap under vacuum: Measurements of laser-induced heating via NV center thermometry, *Appl. Phys. Lett.* **111**, 013101 (2017).
- [45] G. P. Conangla, A. W. Schell, R. A. Rica, and R. Quidant, Motion control and optical interrogation of a levitating single nitrogen vacancy in vacuum, *Nano Lett.* **18**, 3956 (2018).
- [46] G. P. Conangla, R. A. Rica, and R. Quidant, Extending vacuum trapping to absorbing objects with hybrid Paul-optical traps, *Nano Lett.* **20**, 6018 (2020).
- [47] D. S. Bykov, M. Meusburger, L. Dania, and T. E. Northup, Hybrid electro-optical trap for experiments with levitated particles in vacuum, *Rev. Sci. Instrum.* **93**, 073201 (2022).
- [48] J. Janszky and Y. Yushin, Squeezing via frequency jump, *Opt. Commun.* **59**, 151 (1986).
- [49] R. Graham, Squeezing and frequency changes in harmonic oscillations, *J. Mod. Opt.* **34**, 873 (1987).
- [50] C. F. Lo, Squeezing by tuning the oscillator frequency, *J. Phys. A* **23**, 1155 (1990).
- [51] M. Xin, W. S. Leong, Z. Chen, Y. Wang, and S.-Y. Lan, Rapid quantum squeezing by jumping the harmonic oscillator frequency, *Phys. Rev. Lett.* **127**, 183602 (2021).
- [52] E. Bonvin, L. Devaud, M. Rossi, A. Militaru, L. Dania, D. S. Bykov, M. Teller, T. E. Northup, L. Novotny, and M. Frimmer, Hybrid Paul-optical trap with large optical access for levitated optomechanics, [arXiv:2312.10131](https://arxiv.org/abs/2312.10131).
- [53] J.-S. Chen, Ticking near the zero-point energy: Towards 1e-18 accuracy in Al<sup>+</sup> optical clocks, Ph.D. thesis, University of Colorado, 2017.
- [54] J.-S. Chen, S. M. Brewer, C. W. Chou, D. J. Wineland, D. R. Leibbrandt, and D. B. Hume, Sympathetic ground state cooling and time-dilation shifts in an <sup>27</sup>Al<sup>+</sup> optical clock, *Phys. Rev. Lett.* **118**, 053002 (2017).

- [55] S. M. Brewer, J.-S. Chen, A. M. Hankin, E. R. Clements, C. W. Chou, D. J. Wineland, D. B. Hume, and D. R. Leibbrandt,  $^{27}\text{Al}^+$  quantum-logic clock with a systematic uncertainty below  $10^{-18}$ , *Phys. Rev. Lett.* **123**, 033201 (2019).
- [56] M. Teller, V. Messerer, K. Schüppert, Y. Zou, D. A. Fioretto, M. Galli, P. C. Holz, J. Reichel, and T. E. Northup, Integrating a fiber cavity into a wheel trap for strong ion–cavity coupling, *AVS Quantum Sci.* **5**, 012001 (2023).
- [57] E. Bonvin, Hybrid traps for coherent state expansion of a levitated nanoparticle, Doctoral thesis, ETH Zurich, Zurich, 2023.
- [58] See Supplemental Material at <http://link.aps.org/supplemental/10.1103/PhysRevLett.132.253602>, including Refs. [59–64], for details regarding the change of basis, position and velocity measurement, and the model including micromotion.
- [59] B. Hauer, C. Doolin, K. Beach, and J. Davis, A general procedure for thermomechanical calibration of nano/micro-mechanical resonators, *Ann. Phys. (Amsterdam)* **339**, 181 (2013).
- [60] E. Hebestreit, M. Frimmer, R. Reimann, C. Dellago, F. Ricci, and L. Novotny, Calibration and energy measurement of optically levitated nanoparticle sensors, *Rev. Sci. Instrum.* **89**, 033111 (2018).
- [61] E. Joos and A. Lindner, Langevin equation for the parametric oscillator: A model for ion confinement in a radio frequency trap, *Z. Phys. D* **11**, 295 (1989).
- [62] N. W. McLachlan, *Theory and Application of Mathieu Functions* (Dover Publications, New York, 1964).
- [63] J. Meixner and F. W. Schäfke, *Mathieusche Funktionen und Sphäroidfunktionen* (Springer Berlin Heidelberg, Berlin, Heidelberg, 1954).
- [64] M. Abramowitz and I. A. Stegun, *Handbook of Mathematical Functions with Formulas, Graphs, and Mathematical Tables* (Dover, New York, 1964).
- [65] B. Efron, Bootstrap methods: Another look at the Jackknife, *Ann. Stat.* **7**, 1 (1979).
- [66] F. Tebbenjohanns, M. Frimmer, A. Militaru, V. Jain, and L. Novotny, Cold damping of an optically levitated nanoparticle to Microkelvin temperatures, *Phys. Rev. Lett.* **122**, 223601 (2019).
- [67] G. P. Conangla, F. Ricci, M. T. Cuairan, A. W. Schell, N. Meyer, and R. Quidant, Optimal feedback cooling of a charged levitated nanoparticle with adaptive control, *Phys. Rev. Lett.* **122**, 223602 (2019).
- [68] T. Agrenius, C. Gonzalez-Ballester, P. Maurer, and O. Romero-Isart, Interaction between an optically levitated nanoparticle and its thermal image: Internal thermometry via displacement sensing, *Phys. Rev. Lett.* **130**, 093601 (2023).
- [69] F. Tebbenjohanns, M. Frimmer, and L. Novotny, Optimal position detection of a dipolar scatterer in a focused field, *Phys. Rev. A* **100**, 043821 (2019).
- [70] E. E. Wollman, C. U. Lei, A. J. Weinstein, J. Suh, A. Kronwald, F. Marquardt, A. A. Clerk, and K. C. Schwab, Quantum squeezing of motion in a mechanical resonator, *Science* **349**, 952 (2015).
- [71] A. Youssefi, S. Kono, M. Chegnizadeh, and T. J. Kippenberg, A squeezed mechanical oscillator with millisecond quantum decoherence, *Nat. Phys.* **19**, 1697 (2023).
- [72] O. Romero-Isart, Coherent inflation for large quantum superpositions of levitated microspheres, *New J. Phys.* **19**, 123029 (2017).